Structural Engineering and Mechanics, Vol. 30, No. 3 (2008) 263-278
DOI: http://dx.doi.org/10.12989/sem.2008.30.3.263

Static displacement and elastic buckling characteristics of structural pipe-in-pipe cross-sections

M. Sato†

Graduate School of Engineering, Hokkaido University, Sapporo, Japan

M. H. Patel

School of Engineering, Cranfield University, Cranfield, United Kingdom

F. Trarieux

School of Engineering, Cranfield University, Cranfield, United Kingdom

(Received November 23, 2006, Accepted August 19, 2008)

Abstract. Structural pipe-in-pipe cross-sections have significant potential for application in offshore oil and gas production systems because of their property that combines insulation performance with structural strength in an integrated way. Such cross-sections comprise inner and outer thin walled pipes with the annulus between them fully filled by a selectable thick filler material to impart an appropriate combination of properties. Structural pipe-in-pipe cross-sections can exhibit several different collapse mechanisms and the basis of the preferential occurrence of one over others is of interest. This paper presents an elastic analyses of a structural pipe-in-pipe cross-section when subjected to external hydrostatic pressure. It formulates and solves the static and elastic buckling problem using the variational principle of minimum potential energy. The paper also investigates a simplified formulation of the problem where the outer pipe and its contact with the filler material is considered as a 'pipe on an elastic foundation'. Results are presented to show the variation of elastic buckling pressure with the relative elastic modulus of the filler and pipe materials, the filler thickness and the thicknesses of the inner and outer pipes. The range of applicability of the simplified 'pipe on an elastic foundation' analysis is also presented. A brief review of the types of materials that could be used as the filler is combined with the results of the analysis to draw conclusions about elastic buckling behaviour of structural pipe-in-pipe cross-sections.

Keywords: pipe-in-pipe; elastic buckling; stress function; variational method.

1. Introduction

Sub-sea pipelines in deep water are expected to deliver three distinctly different types of performance. First and foremost they need to have collapse resistance to external hydrostatic

† Assistant Professor, Ph.D., Corresponding author, E-mail: tayu@eng.hokudai.ac.jp

pressure in deep water (up to 2000 m). Secondly, the requirement of oil and gas production requires the pipes to have insulating properties to a varying degree depending on the production fluids being carried. Thirdly, in many cases, the weight in water of sub-sea pipelines is a key design requirement. Pipelines laying on the sea bed, or buried just under it require high submerged weight for stability whereas pipelines suspended in the water column require low buoyant weight to reduce surface vessel tension requirements.

Structural pipe-in-pine cross-sections are a possible, efficient design solution to this three-way performance problem. Such cross-sections comprise inner and outer thin walled steel pipes with the annulus fully filled by a filler material with no voids such that the material provides structural support to both the inner and outer pipe walls. The filler can be from a wider variety of materials ranging from plastics through to advanced composites and ceramics. The choice of filler material for optimum collapse strength, insulation and buoyancy leads to design efficiencies which are expected to be important for deep water applications.

Much work has been carried out in this field in recent years. For example, the phenomena of buckle propagation in pipe-in-pipe systems are investigated from the viewpoint of both analytical and experimental aspects by Kyriakides (2002). Oslo and Kyriakides (2003) and Kyriakides and Netto (2004) considered the dynamic propagation and arrest of buckles in pipe-in-pipe systems. Moreover, Han *et al.* (2004) and Kardmateas and Simitses (2005) analytically investigated the buckling of long sandwich cylindrical shells under external pressure. Da Silva (1997) studied the structural properties of multi-layered pipelines. The oil and gas industry has carried out much internal work on pipe-in-pipe cross sections including the conduct of several joint industry projects – see BPP *et al.* (2001) as an example.

On the other hand, it is empirically known that there can be several kinds of local buckling for pipe-in-pipe cross-sections that can not exist in single wall pipes because the core supports both the outer and inner pipes elastically. It is quite important to estimate the buckling strength and the corresponding buckling modes for the structural design of pipe-in-pipe systems; however, previous research has only an dealt with only overall buckling with relatively thin-walled structures and such an interactive buckling phenomenon between the pipes and the core has not been well understood so far.

The purpose of this paper is to investigate the interactive behaviors between the pipes and the thicker core in pipe-in-pipe cross-sections under external hydrostatic pressure in terms of static displacements and elastic buckling characteristics. To do this, the formulations and the elasticity solutions based on the variational principle of minimum potential energy are developed. The effect of transverse shear deformation on the structural properties for this type of composite cross-sections is more significant than that for single wall cross-section especially when the core is relatively thick. In order to evaluate this effect accurately, the core is modeled by using the two-dimensional theory of elasticity.

Distinctive properties of pipe-in-pipe cross-sections are found from investigation of the static displacements. In elastic buckling analysis, the characteristic equations governing buckling are developed in terms of the stiffness and thickness of the core and of the outer and inner pipes. Critical pressures and mode shapes characterizing the elastic buckling phenomena of the pipe-in-pipe cross-section are investigated for various stiffness and thickness parameters. In addition, a simplified formulation for estimating the elastic buckling pressure based on the theory of "Ring on an elastic foundation" by Brush and Almroth (1975) is proposed and its applicability limits are discussed.

Table 1 Young's Modulus of the cores

Core material	Young's modulus range [GPa]
Ceramics	2.5 to 800 GPa
Polymers	25 to 2500 MPa
Advanced composites	30 to 190 GPa

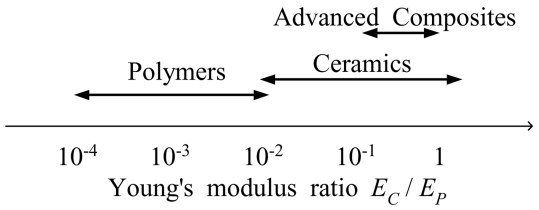

Fig. 1 Ranges of Young's modulus ratio for different material types

2. Mechanical properties of the annulus filler material

A key to the design success of structural pipe-in-pipe cross-sections is the range of materials available for use as the annulus filler. These can range from elastomers and plastics which have the overall characteristic of low elastic modulus but combined with low density (weight) and high insulation performance. At the other extreme of potential filler materials are ceramics which exhibit high elastic modulus but combined with higher densities (weight) and moderate insulation performance. Other material types include advanced composites that have elastic modulus properties around those of ceramics but with different combinations of density and insulation performance.

BPP *et al.* (2001) have given a very comprehensive overview of potential filler material properties by carrying out a survey of over 3000 possible material types. However, for the purposes of this paper, only the elastic moduli of these material types are significant. Table 1 and Fig. 1 present an overview of the range of elastic (Young's) Modulus exhibited by three different material groups in terms of E_c/E_p, the ratio of the Young's Modulus of the material to that of steel.

3. Analytical model of the pipe-in-pipe cross-section

Fig. 2 shows the configuration of a perfectly cylindrical pipe-in-pipe cross-section that is analyzed here. The geometric variables are the thickness of the outer pipe, h_1, that of the inner pipe, h_2, the outer radius, a_1 and the inner radius, a_2. The pipe-in-pipe cross-sections under consideration have an annulus fully filled with a material that provides continuous structural support to both the thin-walled outer and inner pipes. This system is idealized as a two-dimensional plane strain problem for very long pipe lengths. The core material is isotropic and elastic with Young's modulus E_C and Poisson's ratio ν_C. Both the outer and inner pipes are assumed to be very thin compared with their diameters and the thickness of the core (h_1, $h_2 << a_1$, $a_1 - a_2$). For this reason, the outer and inner pipes are modeled as thin-walled rings and the core is treated as a thick hollow cylinder; moreover, the outer and inner surfaces of the core correspond to the middle surfaces of the outer and inner pipes ($r = a_1$, $r = a_2$). Static deformation and elastic buckling behavior are investigated with a uniform external pressure q acting on the outer pipe.

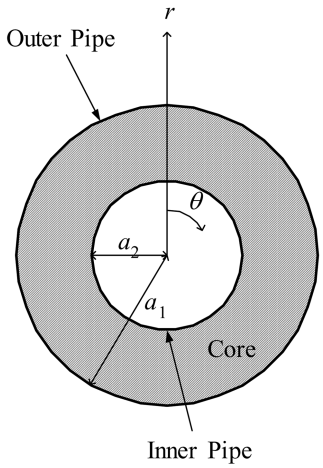

Fig. 2 Geometry of a pipe-in-pipe cross-section

4. Formulation

The governing equation of the core is expressed in polar $(r-\theta)$ coordinates as (see Timoshenko *et al.* 1961)

$$\left(\frac{\partial^2}{\partial r^2}+\frac{1}{r}\frac{\partial}{\partial r}+\frac{1}{r^2}\frac{\partial^2}{\partial \theta^2}\right)\left(\frac{\partial^2 \phi}{\partial r^2}+\frac{1}{r}\frac{\partial \phi}{\partial r}+\frac{1}{r^2}\frac{\partial^2 \phi}{\partial \theta^2}\right)=0 \tag{1}$$

where ϕ is the stress function in the core material. This can be expressed as follows

$$\phi = \phi^{(0)} + \phi^{(1)} \tag{2}$$

where superscript (0) and (1) denotes the circular and noncircular configurations. Under uniform external pressure, $\phi^{(0)}$ and $\phi^{(1)}$ relate to the static and buckled state, respectively.

Displacements of the outer and inner rings in the radial directions u_1 and u_2, and circumferential directions v_1 and v_2 are expressed by circular and noncircular configurations, as

$$u_1 = u_1^{(0)} + u_1^{(1)}, \quad v_1 = v_1^{(1)} \tag{3a}$$

$$u_2 = u_2^{(0)} + u_2^{(1)}, \quad v_2 = v_2^{(1)} \tag{3b}$$

4.1 Circular configuration (Static deformation)

In this case, it is apparent that $\phi^{(0)}$ is a function of only r, that is $\phi^{(0)} = \phi^{(0)}(r)$. Thus, the governing Eq. (1) becomes

$$\left(\frac{d^2}{dr^2}+\frac{1}{r}\frac{d}{dr}\right)\left(\frac{d^2\phi^{(0)}(r)}{dr^2}+\frac{1}{r}\frac{d\phi^{(0)}(r)}{dr}\right)=0 \tag{4}$$

The general solution is obtained as

$$\phi^{(0)}(r) = A^{(0)}\log r + B^{(0)}r^2\log r + C^{(0)}r^2 + D^{(0)} \tag{5}$$

where $A^{(0)}, B^{(0)}, C^{(0)}, D^{(0)}$ are arbitrary constants. The corresponding stress components are

$$\sigma_r^{(0)} = \frac{1}{r}\frac{d\phi^{(0)}(r)}{dr} = A^{(0)}\frac{1}{r^2} + B^{(0)}(1 + 2\log r) + 2C^{(0)} \tag{6a}$$

$$\sigma_\theta^{(0)} = \frac{d^2\phi^{(0)}(r)}{dr^2} = -A^{(0)}\frac{1}{r^2} + B^{(0)}(3 + 2\log r) + 2C^{(0)} \tag{6b}$$

and $\tau_{r\theta}^{(0)} = 0$. Moreover, the strain components for the plane strain problem are derived from the strain-stress relationship as

$$\varepsilon_r^{(0)} = \frac{1}{E_C}\{(1 - \nu_C^2)\sigma_r - \nu_C(1 + \nu_C)\sigma_\theta\}$$

$$= \frac{1 + \nu_C}{E_C}\left[\frac{A^{(0)}}{r^2} + \{1 - 4\nu_C + 2(1 - 2\nu_C)\log r\}B^{(0)} + 2(1 - 2\nu_C)C^{(0)}\right] \tag{7a}$$

$$\varepsilon_\theta^{(0)} = \frac{1}{E_C}\{(1 - \nu_C^2)\sigma_\theta^{(0)} - \nu_C(1 + \nu_C)\sigma_\theta^{(0)}\}$$

$$= -\frac{1 + \nu_C}{E_C}\left[\frac{A^{(0)}}{r^2} + \{(-3 + 4\nu_C) + 2(-1 + 2\nu_C)\log r\}B^{(0)} + 2(-1 + 2\nu_C)C^{(0)}\right] \tag{7b}$$

and $\gamma_{r\theta}^{(0)} = 0$. The radial displacement is easily found by the displacement-strain relationship

$$u^{(0)}(r) = r\varepsilon_\theta^{(0)} = -\frac{1 + \nu_C}{E_C}\left[\frac{A^{(0)}}{r} + \{(-3 + 4\nu_C) + 2(-1 + 2\nu_C)\log r\}B^{(0)}r + 2(-1 + 2\nu_C)C^{(0)}r\right] \tag{8}$$

The continuity conditions between the core and the outer and inner pipes at $r = a_1$ and $r = a_2$ are

$$u^{(0)}(a_1) = u_1^{(0)} \tag{9a}$$

$$u^{(0)}(a_2) = u_2^{(0)} \tag{9b}$$

from Eqs. (8), (9a) and (9b)

$$A^{(0)} = \frac{E_C}{1 + \nu}\frac{a_1^3 a_2^3(a_2 u_1^{(0)} - a_1 u_2^{(0)})}{a_1^4 - a_2^4} \tag{10a}$$

$$C^{(0)} = \frac{E_C}{2(1 - \nu)}\frac{a_1^3 u_1^{(0)} - a_2^3 u_2^{(0)}}{a_1^4 - a_2^4} \tag{10b}$$

and $B^{(0)} = 0$ in the symmetrical stress distribution.

The total potential energy per unit width $U^{(0)}$ can be given by the sum of the strain energy of the core, $U_C^{(0)}$, the strain energies of the outer and inner pipes, $U_{P,1}^{(0)}, U_{P,2}^{(0)}$ and the potential energy Ω by the applied external pressure q, as

$$U^{(0)} = U_C^{(0)} + U_{P,1}^{(0)} + U_{P,2}^{(0)} + \Omega^{(0)} = \int_0^{2\pi} F^{(0)} d\theta \tag{11}$$

where

$$U_C^{(0)} = \frac{1}{2}\int_0^{2\pi}\int_{a_2}^{a_1} (\sigma_r^{(0)}\varepsilon_r^{(0)} + \sigma_\theta^{(0)}\varepsilon_\theta^{(0)}) r\, dr\, d\theta \tag{12a}$$

$$U_{P,1}^{(0)} = \frac{E_P h_1 a_1}{2(1-\nu_P^2)}\int_0^{2\pi} \varepsilon_P^{(1)} d\theta \tag{12b}$$

$$U_{P,2}^{(0)} = \frac{E_P h_2 a_2}{2(1-\nu_P^2)}\int_0^{2\pi} \varepsilon_P^{(2)} d\theta \tag{12c}$$

$$\Omega^{(0)} = -q a_1 u_1^{(0)} \tag{12d}$$

From the principle of least work

$$\frac{\partial F^{(0)}}{\partial u_1^{(0)}} = 0 \tag{13a}$$

$$\frac{\partial F^{(0)}}{\partial u_2^{(0)}} = 0 \tag{13b}$$

Substituting Eqs. (12a)-(12d) into Eqs. (13a) and (13b) gives the following equation in matrix form as

$$\begin{bmatrix} m_{11} & m_{12} \\ m_{21} & m_{22} \end{bmatrix} \begin{Bmatrix} u_1^{(0)} \\ u_2^{(0)} \end{Bmatrix} = \begin{Bmatrix} q a_1 \\ 0 \end{Bmatrix} \tag{14}$$

where

$$m_{11} = \frac{E_C\{a_2^2(2\nu_C - 1) - a_1^2\}}{(a_1^2 - a_2^2)(\nu_C + 1)(2\nu_C - 1)} + \frac{E_P h_1}{a_1(1-\nu_P^2)} \tag{15a}$$

$$m_{12} = m_{21} = \frac{2E_C a_1 a_2}{(a_1^2 - a_2^2)(\nu_C + 1)(2\nu_C - 1)} \tag{15b}$$

$$m_{22} = \frac{E_C\{a_2^2 + a_1^2(2\nu_C - 1)\}}{(a_1^2 - a_2^2)(\nu_C + 1)(2\nu_C - 1)} + \frac{E_P h_1}{a_2(1-\nu_P^2)} \tag{15c}$$

Displacements of the outer and inner rings can be obtained by solving Eq. (14) as

$$u_1^{(0)} = \frac{m_{22} q}{m_{11} m_{22} - m_{12}^2} \tag{16a}$$

$$u_2^{(0)} = -\frac{m_{21} q}{m_{11} m_{22} - m_{12}^2} \tag{16b}$$

3.2 Non-Circular configuration (Elastic buckling)

In order to obtain the periodic displacement in θ, $\phi^{(1)}(r,\theta)$ is assumed as follows

$$\phi^{(1)}(r,\theta) = f_n(r)\cos n\theta \tag{17}$$

where n is a mode number. Substituting Eq. (17) into Eq. (4), we obtain

$$\left(\frac{d^2}{dr^2}+\frac{1}{r}\frac{d}{dr}+\frac{n^2}{r^2}\right)\left(\frac{d^2f(r)}{dr^2}+\frac{1}{r}\frac{df(r)}{dr}+\frac{n^2}{r^2}f(r)\right) = 0 \tag{18}$$

The general solutions are

$$f_1(r) = A_1^{(1)}\frac{1}{r}+B_1^{(1)}r+C_1^{(1)}r^3+D_1^{(1)}r\log r \quad (n=1) \tag{19a}$$

$$f_n(r) = A_n^{(1)}r^{-n}+B_n^{(1)}r^{2-n}+C_n^{(1)}r^{2+n}+D_n^{(1)}r^n \quad (n\geq 2) \tag{19b}$$

where $A_n^{(1)}, B_n^{(1)}, C_n^{(1)}, D_n^{(1)}$ are arbitrary constants. In the case of n = 1 (Eq. (19a)), the corresponding displacement mode represents a rigid body translation. For this reason, Eq. (19b) should be used here.

The corresponding stress components are

$$\sigma_r^{(1)} = \frac{1}{r}\frac{\partial\phi^{(1)}(r,\theta)}{\partial r}+\frac{1}{r^2}\frac{\partial^2\phi^{(1)}(r,\theta)}{\partial\theta^2}$$

$$= -\{A_n^{(1)}n(n+1)r^{-n-2}+B_n^{(1)}(n-1)(n+2)r^{-n}+C_n^{(1)}(n+1)(n-2)r^n+D_n^{(1)}n(n-1)r^{n-2}\}\cos n\theta \tag{20a}$$

$$\sigma_\theta^{(1)} = \frac{\partial^2\phi^{(1)}(r,\theta)}{\partial r^2}$$

$$= \{A_n^{(1)}n(n+1)r^{-n-2}+B_n^{(1)}(n-1)(n-2)r^{-n}+C_n^{(1)}(n+1)(n+2)r^n+D_n^{(1)}n(n-1)r^{n-2}\}\cos n\theta \tag{20b}$$

$$\tau_{r\theta}^{(1)} = -\frac{\partial}{\partial r}\left(\frac{1}{r}\frac{\partial\phi^{(1)}(r,\theta)}{\partial\theta}\right)$$

$$= \{-A_n^{(1)}n(n+1)r^{-n-2}-B_n^{(1)}(n^2+n-2)r^{-n}+C_n^{(1)}n(n+1)r^n+D_n^{(1)}n(n-1)r^{n-2}\}\sin n\theta \tag{20c}$$

The strain components for the plane strain problem are derived by

$$\varepsilon_r^{(1)} = \frac{1}{E_C}\{(1-\nu_C^2)\sigma_r^{(1)}-\nu_C(1+\nu_C)\sigma_\theta^{(1)}\}$$

$$= -\frac{1+\nu_C}{E_C}\{A_n^{(1)}n(n+1)r^{-n-2}+B_n^{(1)}(n-1)(n-4\nu_C-2)r^{-n} \tag{21a}$$

$$+C_n^{(1)}(n+1)(n+4\nu_C-2)r^n+D_n^{(1)}n(n-1)r^{n-2}\}\cos n\theta$$

$$\varepsilon_\theta^{(1)} = \frac{1}{E_C}\{(1-\nu_C^2)\sigma_\theta^{(1)} - \nu_C(1+\nu_C)\sigma_r^{(1)}\}$$

$$= \frac{1+\nu_C}{E_C}\{A_n^{(1)}n(n+1)r^{-n-2} + B_n^{(1)}(n-1)(n+4\nu_C-2)r^{-n} + 2C_n^{(1)}(n+1)(n-4\nu_C+2)r^n + D_n^{(1)}n(n-1)r^{n-2}\}\cos n\theta \tag{21b}$$

$$\gamma_{r\theta}^{(1)} = \frac{2(1+\nu_C)}{E_C}\tau_{r\theta}^{(1)}$$

$$= -\frac{2(1+\nu_C)}{E_C}\{A_n^{(1)}n(n+1)r^{-n-2} + B_n^{(1)}n(n-1)r^{-n} - C_n^{(1)}n(n+1)r^n - D_n^{(1)}n(n-1)r^{n-2}\}\sin n\theta \tag{21c}$$

The radial and circumferential displacement $u(r, \theta)$ and $v(r, \theta)$ can be obtained from the displacement-strain relationship

$$u(r, \theta) = \int \varepsilon_r dr$$

$$= \frac{1+\nu_C}{E_C}\{A_n^{(1)}nr^{-n-1} + B_n^{(1)}(n-4\nu_C+2)r^{1-n} - C_n^{(1)}(n+4\nu_C-2)r^{n+1} - D_n^{(1)}nr^{n-1}\}\cos n\theta + P \tag{22a}$$

$$v(r, \theta) = \int (r\varepsilon_\theta - u)d\theta$$

$$= \frac{1+\nu_C}{E_C}\{A_n^{(1)}nr^{-n-1} + B_n^{(1)}(n+4\nu_C-4)r^{1-n} + C_n^{(1)}(n-4\nu_C+4)r^{n+1} + D_n^{(1)}nr^{n-1}\}\sin n\theta + Q \tag{22b}$$

where P and Q are integral constants. In this problem, the boundary conditions are

$$\text{Outer pipe: } u(a_1, \theta) = u_1^{(1)} = U_1\cos n\theta, \quad v(a_1, \theta) = v_1^{(1)} = V_1\sin n\theta \tag{23a}$$

$$\text{Inner pipe: } u(a_2, \theta) = u_2^{(1)} = U_2\cos n\theta, \quad v(a_2, \theta) = v_2^{(1)} = V_2\sin n\theta \tag{23b}$$

Substituting Eqs. (22a) and (22b) into Eqs. (20) and (21), we obtain

$$\frac{1+\nu_C}{E_C}\begin{bmatrix} na_1^{-n-1} & (n-4\nu_C+2)a_1^{1-n} & -(n+4\nu_C-2)a_1^{n+1} & -na_1^{n-1} \\ na_1^{-n-1} & (n+4\nu_C-4)a_1^{1-n} & (n-4\nu_C+4)a_1^{n+1} & na_1^{n-1} \\ na_2^{-n-1} & (n-4\nu_C+2)a_2^{1-n} & -(n+4\nu_C-2)a_2^{n+1} & -na_2^{n-1} \\ na_2^{-n-1} & (n+4\nu_C-4)a_2^{1-n} & (n-4\nu_C+4)a_2^{n+1} & na_2^{n-1} \end{bmatrix} \begin{Bmatrix} A_n^{(1)} \\ B_n^{(1)} \\ C_n^{(1)} \\ D_n^{(1)} \end{Bmatrix} = \begin{Bmatrix} U_1 \\ V_1 \\ U_2 \\ V_2 \end{Bmatrix} \tag{24}$$

By appling the same procedure as that of the circular configuration mentioned in section 4.1, the total potential energy per unit width due to noncircular configurations, $U^{(1)}$, can be given by the summation of the strain energy of the core, $U_C^{(1)}$, those of the outer and inner pipes, $U_{P,1}^{(1)}, U_{P,2}^{(1)}$ and the potential energy $\Omega^{(1)}$ by the applied external pressure q, as

$$U^{(1)} = U_C^{(1)} + U_{P,1}^{(1)} + U_{P,2}^{(1)} + \Omega^{(1)} = \int_0^{2\pi} F^{(1)} d\theta \tag{25}$$

where

$$U_C = \frac{1}{2}\int_0^{2\pi}\int_{a_2}^{a_1}(\sigma_r^{(1)}\varepsilon_r^{(1)} + \sigma_\theta^{(1)}\varepsilon_\theta^{(1)} + \tau_{r\theta}^{(1)}\gamma_{r\theta}^{(1)})r\,dr\,d\theta \tag{26a}$$

$$U_{P,1}^{(1)} = a_1\int_0^{2\pi}\left[\frac{E_P h_1}{2(1-\nu_P^2)}\left\{\frac{v_1^{(1)\prime}+u_1^{(1)}}{a_1}+\frac{1}{2}\left(\frac{v_1^{(1)}-u_1^{(1)\prime}}{a_1}\right)^2\right\}^2 + \frac{E_P h_1^3}{24(1-\nu_P^2)}\left(\frac{v_1^{(1)\prime}-u_1^{(1)\prime\prime}}{a_1^2}\right)^2\right]d\theta \tag{26b}$$

$$U_{P,2}^{(1)} = a_2\int_0^{2\pi}\left[\frac{E_P h_2}{2(1-\nu_P^2)}\left\{\frac{v_2^{(1)\prime}+u_2^{(1)}}{a_2}+\frac{1}{2}\left(\frac{v_2^{(1)}-u_2^{(1)\prime}}{a_2}\right)^2\right\}^2 + \frac{E_P h_2^2}{24(1-\nu_P^2)}\left(\frac{v_2^{(1)\prime}-u_2^{(1)\prime\prime}}{a_2^2}\right)^2\right]d\theta \tag{26c}$$

$$\Omega^{(1)} = q\int_0^{2\pi}\left\{u_1^{(1)}+\frac{1}{2}(v_2^{(1)^2}-u_1^{(1)\prime}v_1^{(1)}+u_1^{(1)}v_1^{(1)\prime}+u_1^{(1)^2})\right\}d\theta \tag{26d}$$

$$X' \equiv \frac{dX}{d\theta} \qquad (X = u_1, v_1, u_2, v_2) \tag{26e}$$

In order to satisfy equilibrium, $U^{(1)}$ must be stationary. Consequently, the integrand $F^{(1)}$ in Eq. (25) has to satisfy the Euler-Lagrange equations and from Eqs. (25) and (26) give the following equations

$$[\mathbf{M}]\{\mathbf{u}\} = \begin{bmatrix} c_{11}+d_{11} & c_{12}+d_{12} & d_{13} & d_{14} \\ c_{21}+d_{21} & c_{22}+d_{22} & d_{23} & d_{24} \\ d_{31} & d_{32} & c_{33}+d_{33} & c_{34}+d_{34} \\ d_{41} & d_{42} & c_{43}+d_{43} & c_{44}+d_{44} \end{bmatrix}\begin{Bmatrix} U_1\cos n\theta \\ V_1\sin n\theta \\ U_2\cos n\theta \\ V_2\cos n\theta \end{Bmatrix} = \mathbf{0} \tag{27}$$

where

$$c_{11} = \frac{2E_P h_1}{a_1(1-\nu_P^2)}\left\{1+\frac{1}{12}\left(\frac{h_1}{a_1}\right)^2 n^4 - q(n^2-1)\right\} \tag{28a}$$

$$c_{12} = c_{21} = \frac{2E_P h_1}{a_1(1-\nu_P^2)}\left[n\left(1+\frac{1}{12}\left(\frac{h_1}{a_1}\right)^2 n^2\right)\right] \tag{28b}$$

$$c_{22} = \frac{2E_P h_1}{a_1(1-\nu_P^2)}\left[n^2\left\{1+\frac{1}{12}\left(\frac{h_1}{a_1}\right)^2\right\}\right] \tag{28c}$$

$$c_{33} = \frac{2E_P h_2}{a_2(1-\nu_P^2)}\left\{1+\frac{1}{12}\left(\frac{h_2}{a_2}\right)^2 n^4\right\} \tag{28d}$$

$$c_{34} = c_{43} = \frac{2E_P h_2}{a_2(1-\nu_P^2)}\left[n\left(1+\frac{1}{12}\left(\frac{h_2}{a_2}\right)^2 n^2\right)\right] \tag{28e}$$

$$c_{44} = \frac{2E_P h_2}{a_2(1-\nu_P^2)}\left[n^2\left\{1+\frac{1}{12}\left(\frac{h_2}{a_2}\right)^2\right\}\right] \tag{28f}$$

The constants d_{ij} $(i,j=1,2,3,4)$ in the matrix [**K**] are the stiffness coefficients due to core elasticity, which are defined in the Appendix. For a nontrivial solution, the characteristic equation is obtained by

$$\det|\mathbf{K}| = 0 \tag{29}$$

The relationships between the critical load q_{cr} and some parameters, for example E_C/E_P, a_2/a_1 and so on, can be obtained by solving Eq. (29). In detail, the value of n is determined by trial to give the smallest eigenvalues for the given nondimensional parameters of E_C/E_P, ν, a_2/a_1, h_1/a_1 and h_2/a_1.

4. Results and discussion

In this section, analytical results for $h_1/a_1 = h_2/a_1 = 0.01$, $\nu_C = 0.4$ and $\nu_P = 0.3$ regarding both the static deformation and elastic buckling under external fluid pressure are introduced and the effects of the relative stiffness of the core to the pipe, E_C/E_P, and the ratio of the inner radius to the outer one, a_2/a_1, on the structural properties of the pipe-in-pipe cross-sections are discussed in detail.

4.1 Circular configuration (Static deformation)

Figs. 3(a) and (b) show the effects of $a_2/a_1$and E_C/E_P on the normalized radial displacements of the outer pipe, $u_1^{(0)}/u^*$ and that of the inner pipe, $u_2^{(0)}/u^*$; Here u^* is the displacement of the outer pipe without any core given by

$$u^* = \frac{q a_1 (1-\nu_P^2)}{E_P}\left(\frac{a_1}{h_1}\right) \tag{30}$$

In the case of $E_C/E_P < 10^{-5}$, $u_1^{(0)} \approx u^*$ and $u_2^{(0)} \approx 0$ regardless of the core thickness. This means that the outer pipe behaves as if it is single walled. When $E_C/E_P = 10^{-4}$ and 10^{-3}, $u_1^{(0)}$ decreases and $u_2^{(0)}$ increases as the core becomes thinner.

On the other hand, the tendency for the case of $E_C/E_P = 10^{-2}$ is different from that for $E_C/E_P < 10^{-3}$

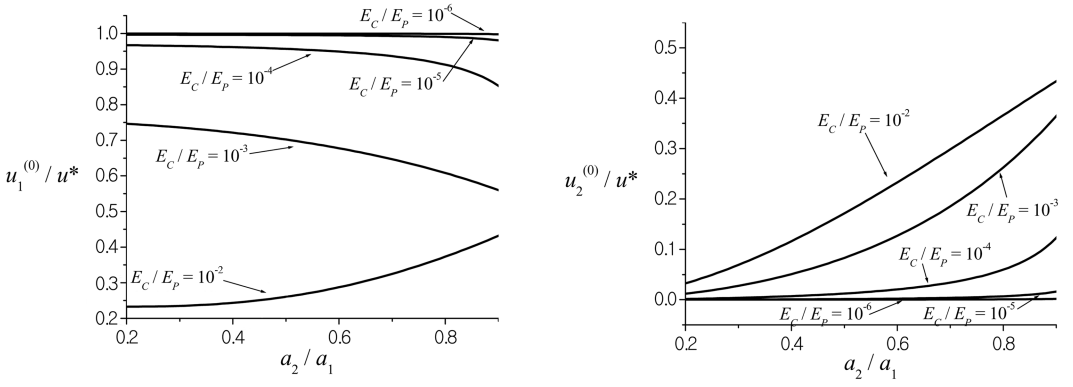

(a) Displacements of the outer pipe (b) Displacements of the inner pipe

Fig. 3 Effects of a_1/a_2 and E_C/E_P on the displacements of pipes

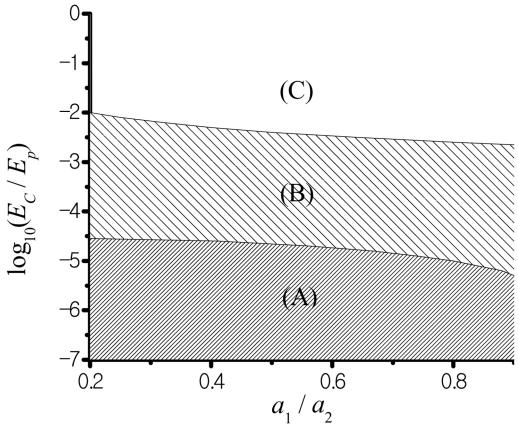

Fig. 4 Structural property (classified by the displacements of the both outer and inner pipes)

mentioned above. $u_1^{(0)}$ almost remains constant up to about $a_2/a_1 = 0.4$ and increases as the core thickness decreases.

Fig. 4 illustrates the structural property classified by the displacements of the both outer and inner pipes. This $a_1/a_2 - \log_{10}(E_C/E_P)$ plane is divided into the following three regions as follows:

(A): The outer pipe behaves as if it is single walled $(u_1^{(0)}/u^* > 0.99)$.

(B): Displacement of the outer pipe decreases as the core becomes thin. This means "thin core = hard core" and the core acts as if it is a linear elastic foundation.

(C): Displacement of the outer pipe increases as the core becomes thin. This means that "thin core = soft core" and pipe-in-pipe cross-section behaves as if it is a "single combined pipe".

For practical ranges of the Young's modulus ratio shown in Fig. 1, the cases of (B) and (C) are applicable. These characteristic properties of pipe-in-pipe cross-sections mentioned above are very different from the behavior of a single walled pipe.

4.2 Non-circular configuration (Elastic buckling)

Fig. 5 shows the normalized critical buckling pressure of the pipe-in-pipe cross-section for practical ranges of the relative stiffness parameter described in Fig. 1; Here q^* is the critical pressure of the outer pipe without any core, given by

$$q^* = \frac{E_p}{4(1-\nu_P^2)} \frac{1}{1+\frac{1}{12}\left(\frac{h_1}{a_1}\right)^2} \left(\frac{h_1}{a_1}\right)^3 \tag{31}$$

In Fig. 5, the solid lines express the critical pressures that can be obtained from Eq. (29) and the dotted lines indicate simplified approximations of the critical buckling pressures based on the theory of a "Ring on an elastic foundation", given by

$$q_{cr} = \frac{1}{12} \frac{n^2-1}{1+\frac{1}{12}\left(\frac{h_1}{a_1}\right)^2} \frac{E_p}{1-\nu_P^2} \left(\frac{h_1}{a_1}\right)^3 + \frac{1}{n^2-1} d_{11} a_1 \tag{32}$$

Eq. (32) is a simple formulation obtained by introducing the influence of the core on the buckling

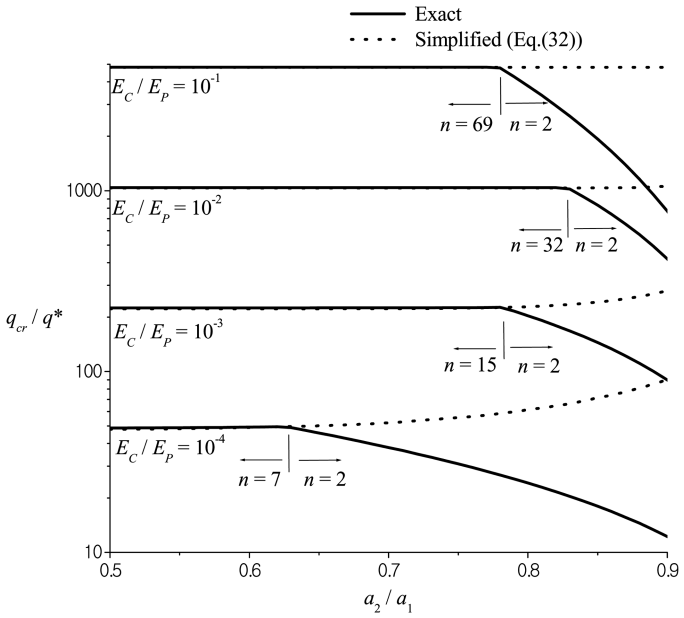

Fig. 5 Critical buckling pressures

characteristics of the outer pipes by treating it as an uncoupled radial spring, that is, a Winkler foundation.

As shown in Fig. 5, the critical buckling pressure q_{cr} increases as E_C/E_P increases. For all cases of $E_C/E_P > 10^{-4}$, when the core thickness is relatively large (i.e., a_2/a_1 is small), it is found from Fig. 5 that the critical buckling pressures are almost constant regardless of the core thickness. In this range, there is extremely close agreement between the exact and the simplified approximation based on the assumption of "Ring on an elastic foundation". Moreover, when the core is relatively hard, higher order buckling modes can occur due to interactions between the core and the outer pipe.

In contrast to this, when the core thickness is small (i.e., a_2/a_1 is large), the buckling modes correspond to $n = 2$ and the critical buckling pressure decreases as the core thickness decreases, as in the case of single wall pipes. It is apparent that the outer and inner pipes and the core behave as a combined pipe in this range. Thus, Fig. 5 indicates that the two buckling phenomena can also occur for these ranges; one is the overall buckling as a combined pipe, and the other is the local buckling of the outer pipe. From the structural design point of view, it should be noted that the crossing points between the line for $n > 2$ and $n = 2$ indicate the optimum core thickness ratio. In addition, as the core elastic modulus becomes smaller, the effect of transverse shear deformation becomes significant. For this reason, the buckling modes correspond to $n = 2$ in spite of the thick core when E_C/E_P is 10^{-4}.

From Fig. 6 to Fig. 8 show the critical elastic buckling modes of the pipe-in-pipe cross-sections. The values of E_C/E_P and a_2/a_1 in these figures are chosen to represent the ranges of applicability in practical design. These figures indicate that the buckling characteristics drastically change as the relative stiffness and the core thickness change. In the following, the structural properties within the ranges of $10^{-4} \le E_C/E_P \le 10^{-2}$ and $0.7 \le a_2/a_1 \le 0.9$ shown in Fig. 6 to Fig. 8 are discussed here.

Higher order buckling modes which correspond to modes greater than 2 are observed when

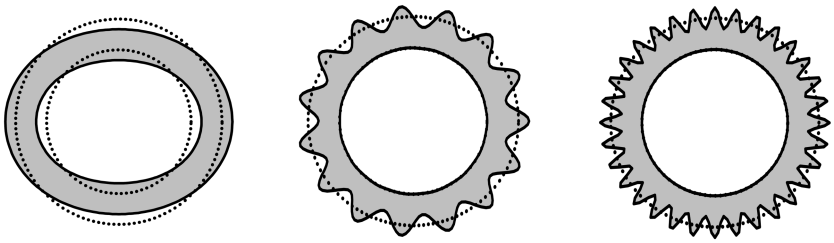

(a) $E_C / E_P = 10^{-4}$ (b) $E_C / E_P = 10^{-3}$ (c) $E_C / E_P = 10^{-2}$

Fig. 6 Buckling modes (a_2/a_1 = 0.7)

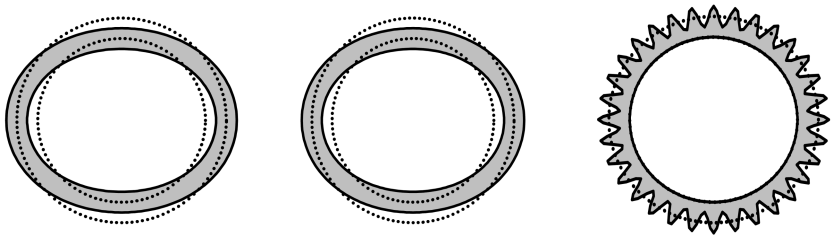

(a) $E_C / E_P = 10^{-4}$ (b) $E_C / E_P = 10^{-3}$ (c) $E_C / E_P = 10^{-2}$

Fig. 7 Buckling modes (a_2/a_1 = 0.8)

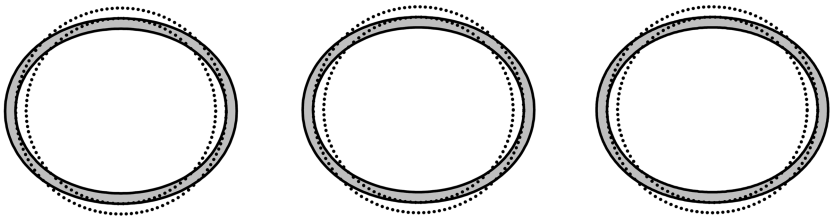

(a) $E_C / E_P = 10^{-4}$ (b) $E_C / E_P = 10^{-3}$ (c) $E_C / E_P = 10^{-2}$

Fig. 8 Buckling modes (a_2/a_1 = 0.9)

$a_2/a_1 = 0.7$ and $E_C/E_P > 10^{-3}$. In these cases, deformations of the inner pipe due to buckling are negligible. This means that the buckling behaviors can be determined only by the material properties and geometries of the outer pipe and the core in this range. Moreover, this corresponds to the fact that there is close agreement between the critical pressure obtained from Eq. (29) and Eq. (32) based on the assumption of "Ring on an elastic foundation" for the parameter ranges shown in Fig. 5. For $E_C/E_P = 10^{-4}$, the pipe-in-pipe cross-section behaves as if it is a single wall pipe regardless of the core thickness.

On the other hand, in the case of n = 2 for small core thickness, not only the outer pipe and the core but also the inner pipe are deformed as a combined pipe.

5. Conclusions

The structural properties of pipe-in-pipe cross-sections which consist of thin-walled outer and

inner pipes and a much thicker core between the outer and inner pipes have been analysed from the viewpoint of static deformation and elastic buckling under uniform external pressure. For practical ranges of material properties and geometries of pipe-in-pipe cross-sections, two typical deformation characteristics can exist; (1) Displacement of the outer pipe decreases as the core becomes thin, which means "thin core = hard core" and the core acts as if it is a linear elastic foundation and (2) Displacement of the outer pipe increases as the core becomes thin, which means that "thin core = soft core" and pipe-in-pipe cross-section behaves as if it is a "single combined pipe".

Similarly, two buckling phenomena can also occur for these ranges; one is the overall buckling as a combined pipe, and the other is the local buckling of the outer pipe. These buckling characteristics strongly depend on the relative stiffness ratio and the thickness of the core. Accordingly, the collapse modes also drastically change corresponding to changes in the relative stiffness and the core thickness.

The analysis presented in this paper is based on the theory of elasticity and has considered pipe-in-pipe cross-sections with a perfectly circular shape. This is a useful formulation for carrying out preliminary design and optimization on pipe-in-pipe systems for underwater applications. It is, of course, the case that plastic behavior will occur especially when the core is thicker and of greater stiffness. In addition, initial imperfections will reduce the critical collapse pressure from that of the idealized structure. Both of these issues need to be the subject of further study.

References

BPP Technical Services LTD. (2001), "Deep water pipe-in-pipe joint industry project".

Brush, D.O. and Almroth, B.O. (1975), *Buckling of Bars, Plates and Shells*, McGraw-Hill, New York.

Da Silva, R.M. (1997), "On the structural mechanics of multi-layered subsea pipelines", *PhD thesis, Department of Mechanical Engineering, University College London*.

Han, J.H., Kardmateas, G.A. and Simitses, G.J. (2004), "Elasticity, shell theory and finite element results for the buckling of long sandwich cylindrical shells under external pressure", *Composites Part B* **35**, 591-598.

Kardmateas, G.A. and Simitses, G.J. (2005), "Buckling of long sandwich cylindrical shells under external pressure", *J. Appl. Mech*., ASME, **72**, 493-499.

Kyriakides, S. (2002), "Buckle propagation in pipe-in-pipe systems: Part I. Experiments", *Int. J. Solids Struct.*, **39**(2), 351-366.

Kyriakides, S. (2002), "Buckle propagation in pipe-in-pipe systems: Part II. Analysis", *Int. J. Solids Struct.*, **39**(2), 367-392.

Kyriakides, S. and Netto, T.A. (2004), "On the dynamic propagation and arrest of buckles in pipe-in-pipe systems", *Int. J. Solids Struct.*, **41**(20), 5463-5482.

Oslo, E. and Kyriakides, S. (2003), "Internal ring buckle arrestors for pipe-in-pipe systems", *Int. J. Non. Mech.*, **38**(2), 267-284.

Timoshenko, S.P. and Gere, J.M. (1961), *Theory of Elastic Stability (second edition)*. McGraw-Hill, New York.

Appendix

The constants d_{ij} $(i,j = 1, 2, 3, 4)$ are defined as follows:

$$d_{ij} = \frac{\tilde{d}_{ij}}{d} \quad (i,j = 1, 2, 3, 4)$$

$$d = (1 + \nu_C)[(3 - 4\nu_C)^2 a_1^{4n+2} a_2^2 - \{8(2\nu_C^2 - 3\nu_C + 1) + n^2\} a_1^{2n+4} a_2^{2n}$$
$$+ 2(n^2 - 1) a_1^{2n+2} a_2^{2n+2} - \{8(2\nu_C^2 - 3\nu_C + 1) + n^2\} a_1^{2n} a_2^{2n+4} + (3 - 4\nu_C)^2 a_1^2 a_2^{4n+2}]$$

$$\tilde{d}_{11} = E_C[\{1 - 2\nu_C + 2n(\nu_C - 1)\}(4\nu_C - 3) a_1^{4n+2} a_2^2 - \{8(1 - \nu_C) + n^2(4\nu_C - 5)\} a_1^{2n+4} a_2^{2n}$$
$$+ 2(n^2 - 1)(2\nu_C - 3) a_1^{2n+2} a_2^{2n+2} + \{8(2\nu_C^2 - 3\nu_C + 1) + n^2\} a_1^{2n} a_2^{2n+4}$$
$$- \{2\nu_C - 1 + 2n(\nu_C - 1)\}(4\nu_C - 3) a_1^2 a_2^{4n+2}]$$

$$\tilde{d}_{12} = \tilde{d}_{21} = -E_C[\{2(1 - \nu_C) + n(2\nu_C - 1)\}(-3 + 4\nu_C) a_1^{4n+2} a_2^2 - n\{4(\nu_C - 1) + n^2\} a_1^{2n+4} a_2^{2n}$$
$$+ 2n(n^2 - 1)(2\nu_C - 3) a_1^{2n+2} a_2^{2n+2} - n\{8(2\nu_C^2 - 3\nu_C + 1) + n^2\} a_1^{2n} a_2^{2n+4}$$
$$+ \{2(\nu_C - 1) + n(2\nu_C - 1)\}(4\nu_C - 3) a_1^2 a_2^{4n+2}]$$

$$\tilde{d}_{13} = \tilde{d}_{31} = -2E_C(\nu_C - 1) a_1^{n+1} a_2^{n+1}[(n - 1)\{4(\nu_C - 1) - n\}(a_1^{2n+2} - a_2^{2n+2})$$
$$+ (n + 1)\{4(\nu_C - 1) + n\} a_1^2 a_2^2 (a_1^{2n-2} - a_2^{2n-2})]$$

$$\tilde{d}_{14} = \tilde{d}_{41} = 2E_C(\nu_C - 1) a_1^{n+1} a_2^{n+1}[(n - 1)\{4(\nu_C - 1) - n\} a_2^{2n+2} + (n + 1)\{2(1 - \nu_C) + n\} a_1^{2n} a_2^2$$
$$+ (n + 1)\{4(\nu_C - 1) + n\} a_1^2 a_2^{2n} + (n - 1)\{2(1 - 2\nu_C) - n\} a_2^{2n+2})]$$

$$\tilde{d}_{22} = E_C[\{1 - 2\nu_C + 2n(\nu_C - 1)\}(4\nu_C - 3) a_1^{4n+2} a_2^2 + n^2(4\nu_C - 3) a_1^{2n+4} a_2^{2n}$$
$$- 2(n^2 - 1)(2\nu_C - 1) a_1^{2n+2} a_2^{2n+2} + \{8(\nu_C - 1)(2\nu_C - 1) + n^2\} a_1^{2n} a_2^{2n+4}$$
$$- \{2\nu_C - 1 + 2n(\nu_C - 1)\}(4\nu_C - 3) a_1^2 a_2^{4n+2}]$$

$$\tilde{d}_{23} = \tilde{d}_{32} = 2E_C(\nu_C - 1) a_1^{n+1} a_2^{n+1}[(n - 1)\{2(2\nu_C - 1) + n\} a_1^{2n+2} - (n + 1)\{4(\nu_C - 1) + n\} a_1^{2n} a_2^2$$
$$+ (n + 1)\{2(2\nu_C - 1) - n\} a_1^2 a_2^{2n} + (n - 1)\{4(1 - \nu_C) - n\} a_2^{2n+2})]$$

$$\tilde{d}_{24} = \tilde{d}_{42} = -2E_C(\nu_C - 1) a_1^{n+1} a_2^{n+1}[(n - 1)\{2(2\nu_C - 1) + n\}(a_1^{2n+2} - a_2^{2n+2})$$
$$+ (n + 1)\{2(2\nu_C - 1) - n\} a_1^2 a_2^2 (a_1^{2n-2} - a_2^{2n-2})]$$

$$\tilde{d}_{33} = E_C[\{2\nu_C - 1 + 2n(\nu_C - 1)\}(4\nu_C - 3) a_1^{4n+2} a_2^2 - \{8(\nu_C - 1)(2\nu_C - 1) + n^2\} a_1^{2n+4} a_2^{2n}$$
$$+ 2(n^2 - 1)(2\nu_C - 3) a_1^{2n+2} a_2^{2n+2} + \{8(1 - \nu_C) + n^2(4\nu_C - 5)\} a_1^{2n} a_2^{2n+4}$$
$$- \{1 - 2\nu_C + 2n(\nu_C - 1)\}(4\nu_C - 3) a_1^2 a_2^{4n+2}]$$

$$\tilde{d}_{34} = \tilde{d}_{43} = E_C[\{2(\nu_C-1)+n(2\nu_C-1)\}(4\nu_C-3)a_1^{4n+2}a_2^2 - n\{8(\nu_C-1)(2\nu_C-1)+n^2\}a_1^{2n+4}a_2^{2n} + 2n(n^2-1)a_1^{2n+2}a_2^{2n+2} - n\{4(\nu_C-1)+n^2\}a_1^{2n}a_2^{2n+4} + \{2(1-\nu_C)+n(2\nu_C-1)\}(4\nu_C-3)a_1^2a_2^{4n+2}]$$

$$\tilde{d}_{44} = E_C[\{2\nu_C-1+2n(\nu_C-1)\}(4\nu_C-3)a_1^{4n+2}a_2^2 + \{8(\nu_C-1)(2\nu_C-1)+n^2\}a_1^{2n+4}a_2^{2n} - 2(n^2-1)(2\nu_C-1)a_1^{2n+2}a_2^{2n+2} - n^2(4\nu_C-3)a_1^{2n}a_2^{2n+4} - \{2\nu_C-1+2n(\nu_C-1)\}(4\nu_C-3)a_1^2a_2^{4n+2}]$$